Core-hole effects on electron energy-loss spectroscopy of Li_2O

N. Jiang and J. C. H. Spence
Department of Physics and Astronomy, Arizona State University, Tempe, Arizona 85287-1504, USA
(Received 2 September 2003; revised manuscript received 24 November 2003; published 18 March 2004)

Excitons in electron-energy-loss spectra (EELS) can be overwhelming in some materials. Here we report EELS from Li_2O for both Li and O *K* edges. Comparison with calculations excluding and including core-hole effects suggests that the one-electron (ground state) band structure theory is not valid for the interpretation of the fine structure in EELS of Li_2O. Using a large angle scattering technique, a core exciton in the band gap can be observed in the *K* edge EELS.

DOI: 10.1103/PhysRevB.69.115112 PACS number(s): 79.20.Uv, 71.35.−y, 71.20.Ps

I. INTRODUCTION

Electron energy-loss spectroscopy (EELS) is a well-developed technique, which has been widely used in studying physical and chemical properties of materials. It offers very high spatial resolution and, as an absorption spectroscopy, probes the density of empty states (DOS). In the one-electron approximation, EELS give the fraction of beam electrons that, in traversing a thin slab, have lost energy to the excitation of a core electron from an initial to an unoccupied final state. By considering the highly localized inner core states and ignoring the energy dependence of the transition matrix, EELS can be qualitatively interpreted as the partial empty DOS projected on a particular atom site.[1] Angle-resolved EELS is also possible, and involves a second projection in momentum space.[2] The interpretation of the fine structure of the EELS spectra of some materials, however, has been controversial for several decades.[3] The presence of a core hole, created by electronic excitation, can modify the DOS of the final states, and produce excitonic states in the band gap. In optical spectra, it has generally been feasible to assign one or more sharp peaks at the onset of absorption to excitons.[4] It has become more common to use a final state approximation (including a core hole) in simulations of EELS spectra, and to emphasis the dominant role of core-hole interactions in the core excitation spectra.[5] However, there is no unambiguous way to distinguish excitons from interband transitions in EELS. This is mostly because the band threshold is not easily identified; until recently predictions of EELS core threshold energies involved an accuracy of about 1 eV.[6] Problems have also been existed in the interpretation of x-ray absorption spectra. An effort was made to establish the band threshold by a combination of x-ray photoelectron spectroscopy and optical-gap data,[7] but the use of an arbitrary shift along the energy axis to yield the best match between the calculated DOS and the observed spectrum is still a general practice.

In insulators, the inclusion of excited electrons and core holes is essential to properly interpret excitation spectra.[8] In this paper, we present an interpretation of experimental EELS spectra for the Li and O *K* edges of Li_2O, including excitonic effects. We then establish that the exciton absorption peak can be distinguished in EELS with the assistance of calculations. The valence excitons of Li_2O have been observed in optical absorption spectra,[9,10] and calculated in the near-gap absorption spectrum.[11] However, these valence excitons are different from the core excitons, which are highly localized around the excited atom due to the localized core holes,[12] and do not contribute to photoconductivity. No study of the core-hole exciton of Li_2O appears to have been reported previously. Additionally, an understanding of the electronic structure of Li_2O is a prerequisite for the study of Li_2O-compounds, such as optical glasses, fast-ionic conductors, solid-state batteries, and blanket breeder materials in nuclear reactors.[13] Although the occupied (core and valence) states have been studied,[14] a probe of the unoccupied states is still needed to obtain a full picture of the electronic structure of Li_2O.

II. EXPERIMENT AND THEORETICAL BACKGROUND

Commercial Li_2O powders were used in this study (Aldrich Chemical Company, Inc.). They were used without further purification. No impurities were apparent in the energy dispersive characteristic x-ray spectra. The crystal structure was confirmed by the electron diffraction from the selected area. The transmission electron microscope (TEM) samples were prepared by blowing the Li_2O powders into dry air, and picking them up using a Cu grid covered with lacy carbon thin film. The sample was then immediately transferred into and observed in a Philips EM400 TEM with a field-emission gun operating at 100 keV and a Gatan parallel EELS system. The energy resolution of the spectrometer is about 0.8 eV (determined by the FWHM of the zero-loss peak). The collection semiangle is about 5 mrad.

Radiation damage is very severe in Li_2O. Thus time-resolved EELS and electron diffraction patterns were obtained first from Li_2O to optimize the experimental conditions. It was found that the damage rate is dependent on the thickness of the sample. In thicker areas (>200 nm), the sample can survive electron irradiation long enough to allow collection of EELS spectra with a meaningful signal-to-noise ratio. Therefore multiple scattering effects must be deconvoluted from the original spectrum in order to obtain the single scattering spectrum, which can be compared with the electronic DOS. In this work, the Fourier-log method was used for deconvolution of the EELS spectra.[15] Additionally, Li_2O can easily react with H_2O and CO_2 in the air to form LiOH and Li_2CO_3. The latter can be easily ruled out by the absence of a C *K* edge in the EELS spectra. The former contamination can also be ignored according to the absence

of the edge shift in the O *K* edge, which can be induced by the appearance of (OH).[16]

For small angle scattering, the dipole selection rule is satisfied, and the EELS intensities of the Li and O *K* edges are simply proportional to the unoccupied Li and O *p*-DOS, respectively. For large angle scattering, however, the dipole selection rule may not be valid, and ''forbidden'' transitions, such as $s \rightarrow s$, must be considered.[17,18] The calculations were carried out using the linearnized augment plane wave (LAPW) method within the local density approximation, as encoded in the WIEN2K (Ref. 19) program. Experimental lattice parameters ($a = 3.086$ Å) of Li_2O were used, without further relaxation in the calculations. For comparison, the calculations were also carried out using the real space multiple scattering (RSMS) approach, as encoded in the FEFF8 (Ref. 20) program.

In the LAPW calculations, no shape approximation was made in terms of potentials. The Coulomb potential is expanded in the forms $\Sigma_{lm} V_{lm}(r) Y_{lm}(\hat{\mathbf{r}})$ within the muffin tin, and $\Sigma_K V_K e^{i\mathbf{K}\cdot\mathbf{r}}$ in the interstitial region. This is solved using multipole potentials and the boundary value problem for a sphere.[21] For the exchange-correlation potential, the generalized gradient approximation (GGA) is employed.[22] The LAPW sphere radii (R) are 0.95 Å for the Li and 1.04 Å for the O. To simulate core hole effects, a $2\times2\times2$ supercell was constructed and the excited Li or O in the supercell was replaced by a Be or F atom, respectively (i.e., the so-called $Z+1$ approximation).[12] Due to the large unit cell, this calculation was very time consuming. In the RSMS calculations, a self-consistent muffin tin potential, which is flat in the interstitial region and otherwise is the sum of overlapping, spherically symmetric potentials, and the ground-state von Barth-Hedin exchange-correlation potential[23] were used. The muffin-tin radii were automatically calculated using the Norman prescription, with about 10% overlap to roughly correct for the nonspherical potentials. The core-hole effects are approximated by the removal of one core electron (Li 1*s* or O 1*s*) to the vacuum states. A small cluster (less than 100 atoms) was constructed using the package ATOM.[24]

III. RESULTS AND DISCUSSION

The deconvoluted experimental EELS of the Li and O *K* edges are shown in Figs. 1(a) and 1(b), respectively. It is seen that the overall fine structure in both the Li and O *K* edges are similar: two sharp peaks (indicated by A and B) followed by broad features (indicated by D) in the high-energy region. The two sharp peaks are at 59.8 and 64.5 eV in the Li *K* edge, and 539.6 and 545.4 eV in the O *K* edge, respectively. The separation between the two peaks, however, is narrower in the Li *K* (~4.7 eV) than in the O *K* edge (~5.8 eV). Meanwhile, the relative intensity of the first peak to the second is much weaker in the Li *K* than in the O *K* edge. The asymmetry of the second peaks in both Li and O are also observed; there is a shoulder (indicated by C) on the high-energy side. Due to the low signal-to-noise ratio and channel-to-channel gain variation of the photodiode array, the small bumps before the edges and the variations of the broad features in the high-energy region cannot be simply interpreted as characteristic peaks. Nevertheless, a deep valley can still be recognized at 551 eV (indicated by an arrow) in the O *K* edge, but not in the Li *K* edge.

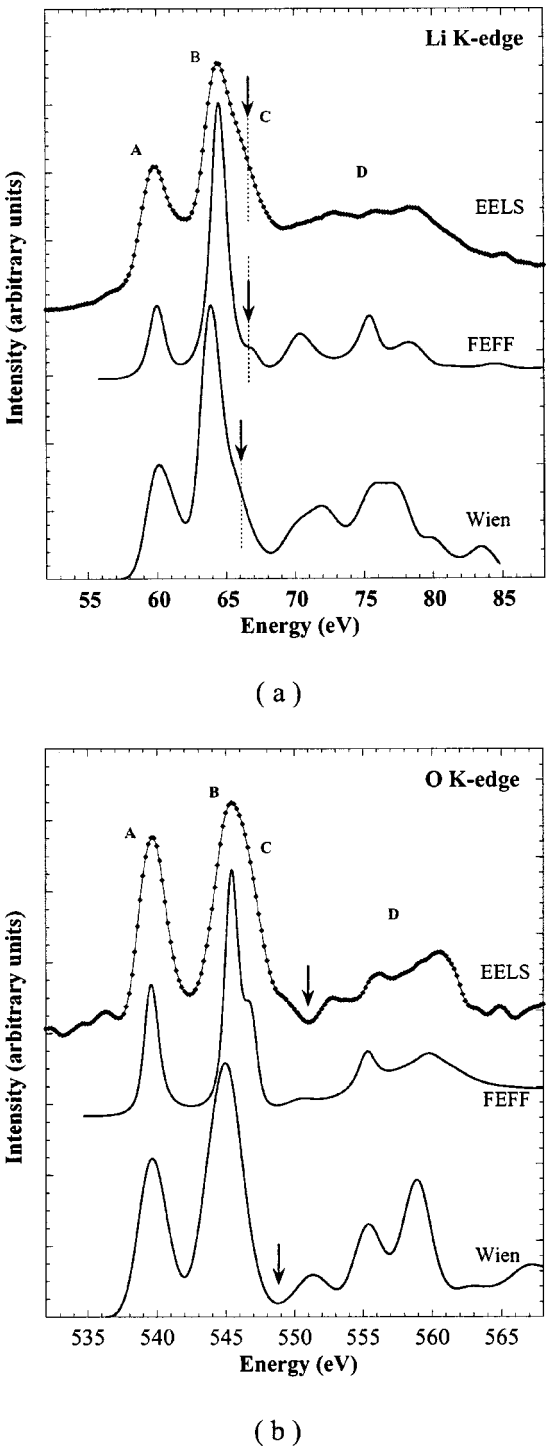

FIG. 1. Comparison of experimental EELS spectra of the (a) Li *K* and (b) O *K* edges with theoretical calculations. The core-hole effects have been considered in calculations.

For comparison, the Li and O *p*-DOS were calculated by including core-hole effects and broadened to 0.8 eV using a Gaussian function. The band edges were aligned to the thresholds of the EELS spectra, which are at the half maxi-

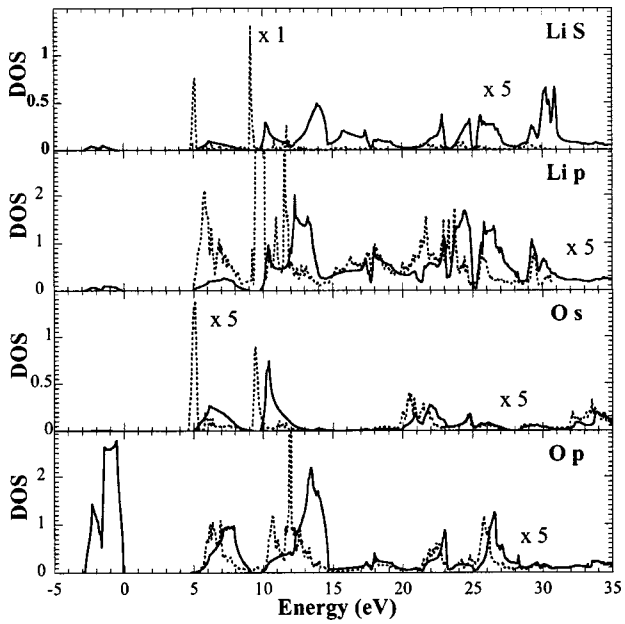

FIG. 2. Calculated partial DOS projected on Li and O atom. The full lines are ground state results, and the dotted lines are including core-hole effects. For comparison, the intensities of unoccupied states have been exaggerated by five times, except Li *s*-DOS with core-hole effects.

mum of the first peak. The justification for this is discussed later. It is seen that the overall features are reproduced by the calculations using both methods. In the RSMS calculations, the positions of two sharp peaks have been exactly reproduced, although the shoulder intensity in the Li *K* is weak in the calculations. On the contrary, the LAPW calculations give a better intensity distribution, but are less accurate in the peak positions. The separations between peak A and B in the Li and O *K* edges are about 1.0 and 0.5 eV less than those in the experimental measurements, respectively. This is probably because the $Z+1$ approximation overestimates the electron-hole interactions. The deep valley observed in the O *K* edge is also reproduced in the LAPW calculation.

Overall, the LAPW method is better than the FEFF in this particular case. However, the former calculation is much more time consuming in order to include the core-hole effects than the FEFF. The weakness of the present version FEFF code is the use of the muffin-tin potential, which is assumed to be zero in the interstitial region. In the near-edge structure calculations, however, the details of the potential in this region are much more important.[25] Nevertheless, the FEFF method can be useful in the large and complicated systems, such as in multicomponent silicates.[26]

The ground state DOS of Li_2O is given in Fig. 2. The valence band is narrow (less than 3 eV) and predominantly O *p* characteristic. The band gap is about 5.0 eV, which is smaller than the optical measurement of 7.99 eV.[10] The unoccupied states approximately consist of three parts: two subbands with a 0.7 eV gap (pseudo gap) followed by continuum states. The lower subband (5.0–9.0 eV) is mainly O character with a minor contribution from Li, while the upper subband (9.7–14.7 eV) is a mixture of Li and O. The continuum part (14.7 eV and above) is dominated by Li *p* characteristic. By comparing the broadened ground state DOS of the Li *p* and O *p* with the experimental EELS of the Li *K* and O *K* edges, the overall features are quite similar: two subbands followed by continuum states. However, the separations between the two subbands are about 5.7 in the Li and 6.1 eV in the O, which are slightly larger than the experimental EELS results. Most importantly, the shoulders of the second subbands are on the low-energy sides, which are opposite to the experimental EELS and the calculations including core-hole effects. Except for this discrepancy, it seems that the ground state DOS does reproduces the fine structure of the experimental EELS at poor energy resolution.

To understand the excitonic effects on the EELS intensities, the unoccupied DOS including electron-hole interactions are also compared in Fig. 2. It is seen that the unoccupied DOS are completely different between the calculations without and with core-hole effects. The most striking difference in the Li *p*-DOS is that the intensity of the lower subband is significantly increased under the electron-hole attraction; a sharp peak occurs at 1 eV above the band edge. Additionally, a sharp peak also appears within the 0.7 eV pseudogap and several sharp peaks in the upper subband. These strong peaks can be interpreted as excitonic excitations, but they cannot be separated from the interband excitations except the one in the pseudogap. However, these excitonic excitations dominate the two major peaks (peaks A and B) of the Li *K* edge [Fig. 1(a)]. Therefore, it is reasonable to assign these two peaks to the excitonic excitations rather than the interband transitions. A better spectrometer with higher energy resolution should be able to distinguish these excitonic peaks. At higher energy, on the contrary, the excitonic effects are relatively weak, and thus the EELS intensity can be interpreted as excitonically enhanced interband transitions.

The excitonic effects on the O *K* edge, on the contrary, only alter the intensity distribution within the sub-bands, and continuum states. Therefore, the fine structure in the O *K* edge is an excitonically enhanced interband transition. The weak excitonic effect on the O *K* edge is due to the electron-hole interaction being screened by the high density of valence electrons. The experimental evidence for different excitonic effects on the Li and O *K* edge comes from the fact that the change of the separation between the two major peaks is larger in the Li *K* than in the O *K* edge (Fig. 1). By comparing with the ground state DOS, it is about 2.0 eV narrow in the calculation including the core-hole effects in the Li *K*, while it is only about 0.8 eV in the O *K*. The electron-hole attraction produces a strong sharp peak in the pseudo gap in the Li *p*-DOS, but not in the O *p*-DOS. As a result, the position of the second peak of the Li *K* edge shifts toward lower energy more than that of the O *K* edge.

In both the Li and O *p*-DOS, no exciton peak is observed below the band edge. Therefore, the thresholds of the *K* edge excitation spectra given in Fig. 1 are justified, although the excitonic excitations dominate at least the first two peaks of the Li *K* edge. However, in the Li and O *s*-DOS, the exciton peak is observed right on the band edge (Fig. 2). This exciton has the lowest energy, but it has *s* symmetry, and the transi-

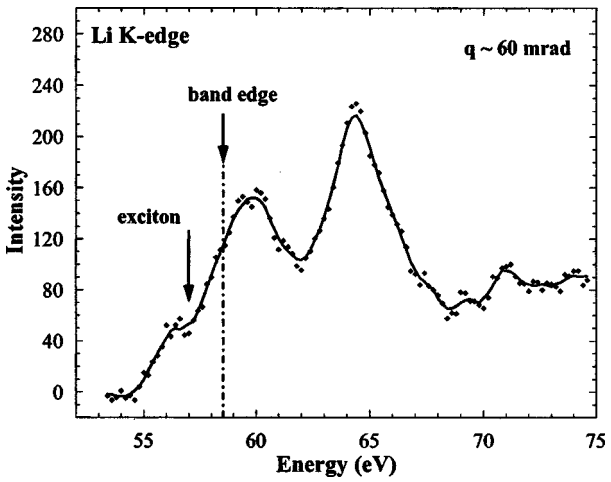

FIG. 3. Li K-edge recorded at large scattering angle ($q \sim 60$ mrad). The chained line represents the band edge.

tion $s \rightarrow s$ is forbidden. Therefore, under the dipole selection rule, either the Li or O K edge cannot see this exciton.

However, in EELS experiments the restriction of the dipole selection rule can be lifted if the spectrum is recorded at a large scattering angle (i.e., $qr \sim 1$). Assuming radius of the core state $r \sim a_0/Z^*$, where a_0 is the Bohr radius and Z^* ($\approx Z - 0.3$ for K edges) is the effective nuclear charge,[27] the dipole conditions should prevail for scattering angle $\theta \ll \theta_d \sim 30$ mrad for Li K-edge excitation by 100 keV electrons. Figure 3 shows the EELS spectrum of the Li K-edge recorded using a 5 mrad (semiangle) collection aperture at a scattering angle of about 60 mrad by moving the diffraction pattern across the spectrometer entrance aperture using diffraction alignment coil.[28] A small peak is observed at about 1.5 eV below the band edge. This peak is due to the excitonic excitation from the Li 1s to an exciton of s symmetry, which is at the band edge in the Li s-DOS (Fig. 2). The broad peak of this exciton results from instrumental broadening, in which the FWHM of the zero-loss peak is about 2 eV. Under the same experimental conditions, the EELS spectrum of the O K edge cannot be obtained because of the low signal-to-noise ratio.

In summary, we have interpreted the fine structure of the Li K and O K-edge EELS in Li_2O with the assistance of band structure calculations including core-hole effects. In addition, the core exciton in the band gap has also been observed using large angle scattering technique. In this ionic insulator, the interactions between electron and core hole completely alter the unoccupied ground state DOS. The ground state DOS interpretation is not long valid. However, the appearance of the two subbands in the ground state unoccupied DOS can easily lead to the opposite conclusion, especially when the energy resolution of the spectrometer is poor.

ACKNOWLEDGMENT

This work is supported by NSF Grant No. DMR-0245702.

[1] M. Inokuti, Rev. Mod. Phys. **43**, 297 (1971).
[2] R. D. Leapman, P. L. Fejes, and J. Silcox, Phys. Rev. B **28**, 2361 (1983); P. E. Batson and M. F. Chisholm, *ibid.* **37**, 635 (1983); N. Nucker, H. Romberg, X. X. Xi, J. Fink, B. Gegenheimer, and Z. X. Zhao, *ibid.* **39**, 6619 (1989); N. Jiang, B. Jiang, J. C. H. Spence, R. C. Yu, S. C. Li, and C. Q. Jin, *ibid.* **66**, 172502 (2002).
[3] R. Buczko, C. Duscher, S. J. Pennycook, and S. T. Pantelides, Phys. Rev. Lett. **85**, 2168 (2000), and references therein.
[4] For reviews see J. C. Phillips, *Fundamental Optical Spectra of Solids, in Solid State Physics* (Academic Press, New York, 1966), Vol 18.
[5] E.g., A. J. Scott, R. Brydson, M. MacKenzie, and A. J. Craven, Phys. Rev. B **63**, 245105 (2001); Y. Xu, Y. Chen, S. Mo, and W. Y. Ching, *ibid.* **65**, 235105 (2002); B. Jiang, N. Jiang, and J. C. H. Spence, J. Phys.: Condens. Matter **15**, 1299 (2003).
[6] D. R. Hamann and D. A. Muller, Phys. Rev. Lett. **89**, 126404 (2002).
[7] S. T. Pantelides, Phys. Rev. B **11**, 2391 (1975).
[8] E. L. Shirley, Phys. Rev. Lett. **80**, 794 (1998).
[9] K. Uchida, K. Noda, T. Tanifuji, Sh. Nasu, T. Kirihara, and A. Kikuchi, Phys. Status Solidi A **58**, 557 (1980).
[10] Y. Ishii, J. Murakami, and M. Itoh, J. Phys. Soc. Jpn. **68**, 696 (1999).
[11] S. Albrecht, G. Onida, and L. Reining, Phys. Rev. B **55**, 10 278 (1997).
[12] H. P. Hjalmarson, H. Buttner, and J. D. Dow, Phys. Rev. B **24**, 6010 (1981).
[13] E.g., C. E. Johnson, K. R. Kummerer, and E. Roth, J. Nucl. Mater. **155–157**, 188 (1988), and references therein.
[14] L. Liu, V. Henrich, W. P. Ellis, and I. Shindo, Phys. Rev. B **54**, 2236 (1996), and references therein.
[15] D. W. Johnson and J. C. H. Spence, J. Phys. D **7**, 771 (1974).
[16] S. Tanaka, M. Taniguchi, and H. Tanigawa, J. Nucl. Mater. **283-287**, 1405 (2000).
[17] D. K. Saldin and J. M. Yao, Phys. Rev. B **41**, 52 (1990).
[18] H. Ma, S. H. Lin, R. W. Carpenter, and O. F. Sanky, J. Appl. Phys. **68**, 288 (1990).
[19] P. Blaha, K. Schwarz, G. K. H. Madsen, D. Kvasnicka, and J. Luitz, WIEN2K, An Augmented Plane Wave + Local Orbitals Program for Calculating Crystal Properties (Karlheinz Schwarz, Tech. Universität Wien, Austria), 2001.
[20] A. L. Ankudinov, B. Ravel, J. J. Rehr, and S. D. Conradson, Phys. Rev. B **58**, 7565 (1998).
[21] M. Weinert, J. Math. Phys. **22**, 2433 (1981).
[22] J. P. Perdew, S. Burke, and M. Ernzerhof, Phys. Rev. Lett. **77**, 3865 (1996).
[23] U. von Barth and L. Hedin, J. Phys. C **5**, 1629 (1972).
[24] URL http://feff.phys.washington.edu/~ravel/software/atoms/
[25] J. J. Rehr and R. C. Albers, Rev. Mod. Phys. **72**, 621 (2000).
[26] N. Jiang, J. Qiu, and J. C. H. Spence, Phys. Rev. B **66**, 054203 (2002).
[27] R. F. Egerton, *Electron Energy-Loss Spectroscopy in Electron Microscope* (Plenum Press, New York, 1996), pp. 230–233.
[28] J. M. Auerhammer and P. Rez, Phys. Rev. B **40**, 2024 (1998).